Supplement of Atmos. Chem. Phys., 18, 8097–8112, 2018
https://doi.org/10.5194/acp-18-8097-2018-supplement

Atmospheric Chemistry and Physics
Open Access
EGU

Supplement of

Insight into global trends in aerosol composition from 2005 to 2015 inferred from the OMI Ultraviolet Aerosol Index

Melanie S. Hammer et al.

Correspondence to: Melanie S. Hammer (melanie.hammer@dal.ca)

Supplement

1. Comparison of simulated and OMI SO_2 and NO_2 columns

We calculate the trends in simulated and OMI SO_2 and NO_2 columns (Figures S1 and S2) to evaluate our GEOS-Chem simulation. There is broad consistency between the trends in our simulated SO_2 and NO_2 columns with those from OMI. There are negative trends in both OMI and simulated SO_2 columns over most of North America, Europe, northern South America, central Africa, and east China. There is a mixture of negative and positive trends in SO_2 over North Africa. There are positive trends in SO_2 over southern South America, southern Africa, the Middle-East, India, most of China, and Australia. The trends in NO_2 columns correspond to the trends in SO_2 columns in almost all regions except for eastern China, which shows positive trends in NO_2 columns for both the simulation and OMI.

2. Comparison of simulated and satellite AOD

Figure S3 shows the trends in GEOS-Chem and satellite AOD for 2005-2015 filtered based on coincident OMI pixels with persistent cloud fraction greater than 5%. Overall the trends in simulated AOD are consistent with the range of trends in satellite AOD. The GEOS-Chem AOD (Figure S3a) shows negative trends in AOD over the eastern United States and West Africa, and positive trends over the western United States, the Middle-East, India, and most of China. Figure S3b shows the trends in AOD from MISR. Significant negative trends are apparent over the eastern United States, Europe, central South America, parts of North Africa, West Africa, and Mongolia/Inner Mongolia. There are small positive trends over west and central United States, parts of South America, parts of North Africa, southern Africa, parts of the Middle-East, parts of China, and Australia, with stronger positive trends over India. AOD from MODIS Dark Target (Figure S3c) shows negative trends over eastern United States, Europe, and central South America, with small positive trends over southern Africa, most of Asia, and Australia, and stronger positive trends over Canada, southern South America, India, and over Central Asia between the Caspian Sea and the Aral Sea. Figure S3d shows the trends in AOD from MODIS Deep Blue. There small negative trends over eastern United States, central South America, Europe, parts of North Africa and West Africa, with stronger negative trends over the Indo-Gangetic Plain and Mongolia/Inner Mongolia. There are positive trends over southern Africa, most of Asia, and Australia, and stronger

positive trends over Canada, southern South America, parts of the Middle-East, India, and over Central Asia between the Caspian Sea and the Aral Sea. Figures S3e and S3f show the trends in AOD from the OMI OMAERUV algorithm at 388 nm and 500 nm, respectively. Significant negative trends are apparent for both wavelengths over central South America, West Africa, the Indo-Gangetic Plain, and Mongolia/Inner Mongolia. Negative trends over Europe and parts of North Africa are more pronounced in the OMI AOD at 388 nm (Figure S3e) than at 500 nm (Figure S3f). There are small positive trends over west and central United States, parts of South America, parts of North Africa, southern Africa, parts of China, and Australia, with stronger positive trends over Canada, India, and over Central Asia between the Caspian Sea and the Aral Sea.

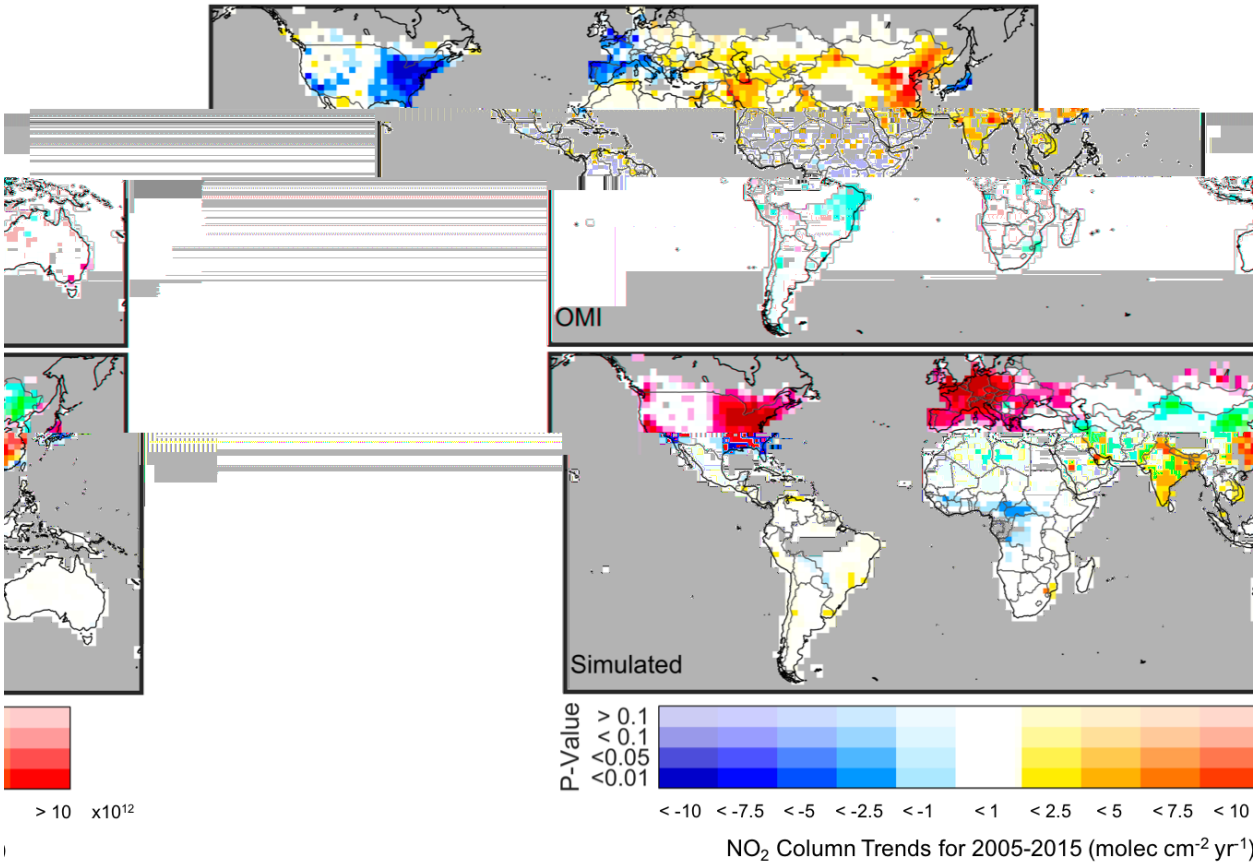

Figure S1: Trends in OMI (top panel) and GEOS-Chem (bottom panel) NO_2 columns calculated from the Generalized Least Squares regression of monthly time series values over 2005-2015. The OMI NO_2 columns are from NASA's OMNO2 version 2.1 product. The opacity of the colors indicates the statistical significance of the trend. Gray indicates persistent cloud fraction greater than 5%.

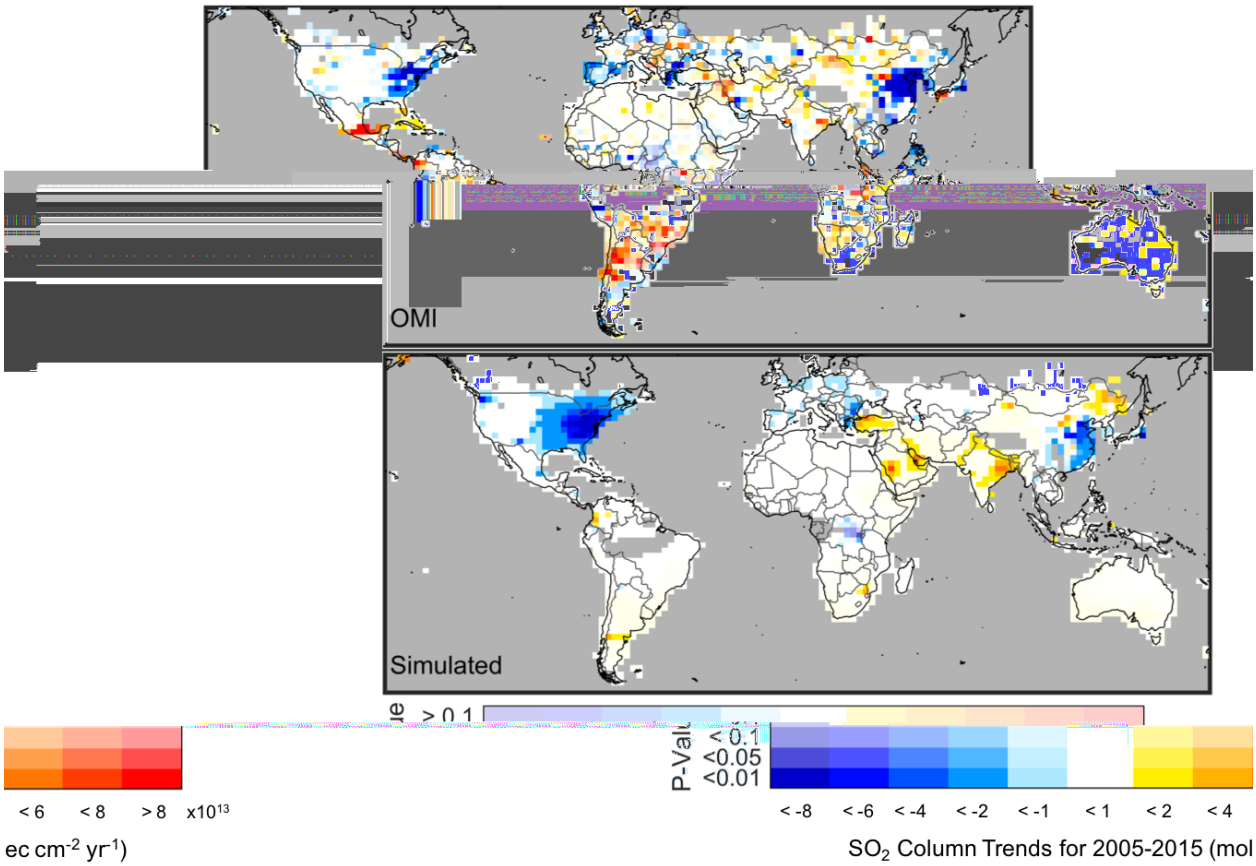

Figure S2: Trends in OMI (top panel) and GEOS-Chem (bottom panel) SO_2 columns calculated from the Generalized Least Squares regression of monthly time series values over 2005-2015. The OMI SO_2 columns are from NASA's $OMSO_2$ version 1.2.0 product. The opacity of the colors indicates the statistical significance of the trend. Gray indicates persistent cloud fraction greater than 5%.

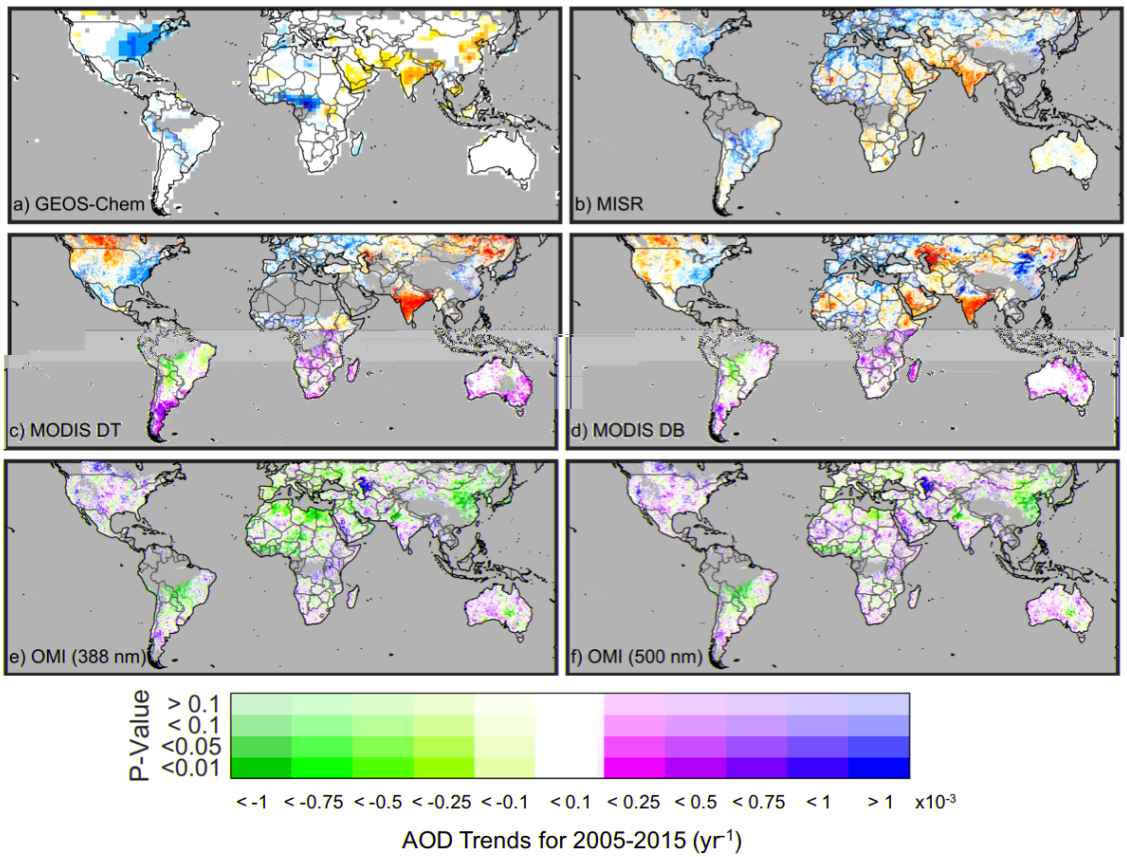

Figure S3: Trends in aerosol optical depth from a) GEOS-Chem (550 nm), b) MISR v22 (550 nm), c) MODIS Terra collection 6 Dark Target algorithm (550 nm), d) the MODIS Terra collection 6 Deep Blue algorithm (550 nm), and the OMI OMAERUV algorithm for e) 388 nm and f) 500 nm. The GEOS-Chem simulation is sampled coincidently with the OMI UVAI product. The trends are calculated from the Generalized Least Squares regression of monthly time series values over 2005-2015. The opacity of the colors indicates the statistical significance of the trend. Gray indicates persistent cloud fraction greater than 5%.